DTD 5
ARTICLE IN PRESS

Journal of South American Earth Sciences xx (xxxx) 1–15

Journal of South American Earth Sciences
www.elsevier.com/locate/jsames

Weathering profiles in granites, Sierra Norte (Córdoba, Argentina)

Alicia Kirschbaum[a,c,*], Estela Martínez[b], Gisela Pettinari[d], Silvana Herrero[b]

[a]CONICET
[b]CIGES, Universidad Nacional de Córdoba. Av. Vélez Sarsfield 299. 5000 Córdoba
[c]CIUNSa, IBIGEO, Museo de Ciencias Naturales, Mendoza 2 - 4.400 - Salta.
[d]CIMAR, Universidad Nacional del Comahue, Buenos Aires 1.400 - 8300 Neuquén

Accepted 15 June 2005

Abstract

Two weathering profiles evolved on peneplain-related granites in Sierra Norte, Córdoba province, were examined. Several weathering levels, of no more than 2 m thickness, were studied in these profiles. They had developed from similar parent rock, which had been exposed to hydrothermal processes of varying intensity. Fracturing is the most notable feature produced by weathering; iron oxides and silica subsequently filled these fractures, conferring a breccia-like character to the rock. The clay minerals are predominantly illitic, reflecting the mineral composition of the protolith. Smaller amounts of interstratified I/S RO type are also present, as well as scarce caolinite + chlorite that originated from the weathering of feldspar and biotite, respectively. The geochemical parameters define the weathering as incipient, in contrast to the geomorphological characteristics of Sierra Norte, which point to a long weathering history. This apparent incompatibility could be due to the probable erosion of the more weathered levels of the ancient peneplains, of which only a few relicts remain. Similar processes have been described at different sites in the Sierras Pampeanas. Reconstruction and dating of the paleosurfaces will make it possible to set time boundaries on the weathering processes studied and adjust the paleographic and paleoclimatic interpretations of this great South American region.

Keywords: Granites; Sierras Pampeanas; Weathering profiles

Resumen

En la Sierra Norte de Córdoba se reconocieron perfiles de meteorización desarrollados sobre granitos vinculados a peneplanicies. Estos perfiles no superan los 2 m de potencia en los que se reconocieron varios niveles meteorización, a partir de una roca madre similar, que estuvo expuesta a procesos hidrotermales de diferente intensidad. El rasgo más destacado producido por la meteorización es la fracturación; estas fracturas fueron luego rellenadas por óxidos de hierro y cuarzo microcristalino, que confieren a la roca un carácter brechoide. Los minerales de arcilla son predominantemente illíticos, reflejando la composición mineralógica del protolito; subordinadamente están presentes interestratificados I/S tipo R0 en forma escasa caolinita + clorita, estas últimas originadas por la meteorización de feldespatos y biotita, respectivamente. Los parámetros geoquímicos de la meteorización la definen como incipiente, en contraposición con las características geomorfológicas de la Sierra Norte, que indican un relieve resultante de una larga historia de meteorización. Esta aparente incompatibilidad podría deberse a la probable erosión de los niveles más meteorizados de antiguas peneplanicies, de las que se conservan sólo algunos relictos. Procesos similares fueron descriptos en diferentes puntos de las Sierras Pampeanas. La reconstrucción de las paleosuperficies y su datación permitirá acotar en el tiempo los procesos de meteorización estudiados, así como ajustar las interpretaciones paleogeográficas y paleoclimáticas de esta extensa región de Sudamérica.

1. Introduction

Most outcropping rocks are subject to conditions that differ markedly from those prevalent during their formation. Weathering consists of thermodynamic readjustment of these rocks to surface conditions.

* Corresponding author. Museo de Ciencias Naturales, Universidad Nacional de Salta, Mendoza 2, 4400-Salta, Argentina.
E-mail address: alikir@unsa.edu.ar (A. Kirschbaum).

0895-9811/$ - see front matter © 2005 Published by Elsevier Ltd.
doi:10.1016/j.jsames.2005.06.001

Environmental conditions change over the geologic time scale, and these variations potentially can be recorded in weathering profiles. Subsequently, erosional processes ensure that only relicts of this weathering history remain, and many features are undoubtedly lost forever. Nevertheless, reconstruction of continental paleosurfaces and an understanding of the weathering processes that formed them constitute valid tools for the investigation of paleoenvironmental problems. In addition, these ancient surfaces are important indicators of global changes (Thiry et al., 1999).

Riggi and Feliu de Riggi (1964) undertook one of the first investigations of rock weathering in Argentina on Cretaceous basalts in Misiones. Their study provides a detailed description of the physical, mineralogical, and geochemical changes produced in different profiles of the region. Iñiguez et al. (1990) describe the paleosoils of the Tandilia System, Buenos Aires Province, in a careful analysis of the petrography, clay mineralogy, and geochemical evolution of various profiles stratigraphically assigned to the Cambrian period.

In the Sierras Pampeanas (SP), previous workers have outlined the weathering of Sierra Grande, Córdoba (Roman Ross et al., 1998; O'Leary et al., 1998), where indications of incipient weathering were defined. Similar degrees of weathering were also found in Sierra Norte, Córdoba (Kirschbaum et al., 2000; Kirschbaum et al., 2002) and Sierra del Aconquija, Tucumán (Kirschbaum, 2002).

The geomorphological features of Sierra Norte encouraged us to find well-developed profiles. Our research goals were to recognize the mineralogical and geochemical effects of weathering in granitic rocks. Our final goal is to attain a better understanding of the processes of rock destruction under surface conditions, which constitutes the first step in sediment production.

2. Geological setting

The SP emerge as a group of southerly directed mountain chains in central and northwestern Argentina. The mountain blocks, separated by tectonic valleys, resulted from uplift and tilt on reverse faults during an Upper Tertiary stage of the Andean orogeny (Rapela et al., 1998). A division between eastern and western SP has been recorded (Caminos, 1979). The eastern SP correspond to an orogen generated during the Proterozoic, with a collision next to the Precambrian-Cambrian limit that gave rise to the magmatism and metamorphism of this age (Ramos, 1999). The Sierra Norte represents the easternmost emergent block of the eastern SP system. It is the only range of this unit oriented NE-SW and is bounded by structures that separate this uplifted block from the surrounding young sediment-covered plains. Lucero (1969, 1979) accurately mapped and described the major and most representative lithological units in the region.

The Sierra Norte batholith intruded a dominantly metasedimentary basement of Precambrian-Cambrian age (K/Ar: 598 ± 20, 517 ± 15 My, Castellote, 1985). The scarce basement outcrops appear as roof-pendant septa within the plutonic rocks, and the contacts between metasedimentary rocks and granitoids are generally fault bounded. The basement is mainly composed of quartzo feldspathic-biotite or sericite-chlorite schists and cordieritic cornubianites, evincing low pressure thermal metamorphism (Kirschbaum et al., 1997).

Local relicts of preintrusive quartz arenites with high textural and mineralogical maturity, forming part of a collapse breccia, have been described in the northern area (Millone et al., 1994). Regional series of enclave-rich granodiorite-monzogranite, locally intruded by a large dacite-rhyolite porphyry stock, prevail in the northern region. These units were subsequently intruded by highly evolved granitoids (miarolitic monzogranites, granite porphyries, and aplite dykes), whose emplacement was controlled by old regional structures (Lira et al., 1997). A porphyry-style hydrothermal alteration system associated with the dacite-rhyolite intrusion also has been identified (Lira et al., 1995). The effect of this alteration is visible in the rocks immediately surrounding the stock.

The magmatism in the southern region of the batholith is predominantly granitic, with scarce grandiorites whose field ratios suggest a subsequent setting. All the rocks are enclave rich, and aplites are frequent (Kirschbaum et al., 1997).

Geochronological data suggest that that the main magmatic activity in Sierra Norte reached its peak in the Lower Ordovician (494 ± 11 My) (Rapela et al., 1991). There is no geochronological information on the few sedimentary rocks in Sierra Norte. Lucero (1969) describes La Lidia Formation arkosic psammites and psephites in two meridian belts in the western sector of the sierra, tentatively assigning them to the Upper Cambrian.

In the Cerro Colorado area (Fig. 1), a continental succession of sandstones with interbedded conglomerates lies with nonconformity on a granitic basement. There is insufficient information about the age of these sedimentary rocks. A post-Cambrian-Triassic age is suggested on the basis of petrographic and geomorphological evidence (Herrero et al., 1998). Quaternary sediments rest directly on the granitic basement in topographic lows, surrounding Sierra Norte on the east and west (Fig. 1).

3. Geomorphological setting

One of the most notable features of the Sierra Norte Massif is the presence of three topographic highs, each located at different heights (500, 700, and 900 m above sea level) and separated by abrupt escarpments. These slope variations limit areas where the hills have similar heights, with flat tops and generally convex slopes (Herrero, 2000). Dome-shaped hills, corestone or boulder tors, inselbergs,

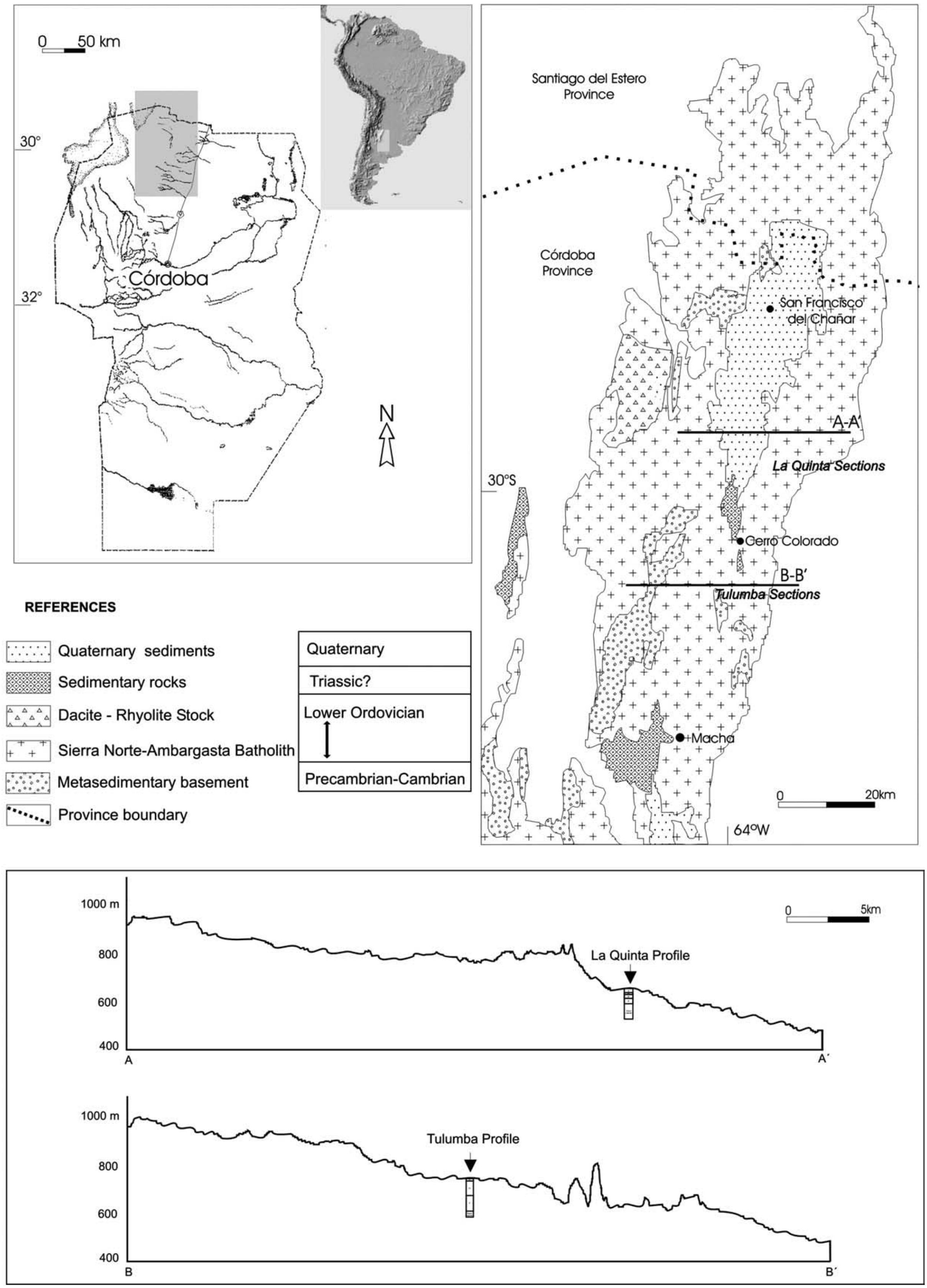

Fig. 1. Sketch of Sierra Norte with the localization of profiles. Sections AA′ and BB′ show the altitude and peneplanized relief of this unit.

and silcretes with polygonal cracks are observed in many localities. These similar denudation features indicate a common morphogenetic origin for Sierra Norte. Fluvial erosion, which postdates the formation of these landscapes, severely dissected the surfaces and often conceals the distinctive characteristics.

Likewise, peneplains with geomorphological characteristics similar to Sierra Norte have been identified in the Sierras Ventania and Tandilia (Buenos Aires province; Rabassa et al., 1995) and Sierra Chica (Córdoba; Cioccale, 1999). The regional character of these extensive geoforms can be inferred from these observations.

The present climatic conditions in Sierra Norte classify it as semidesert, with less than 700 mm/year rainfall. Thus, the area corresponds to a typically semiarid morphogenetic region, where the dominant processes are mechanical and subordinate chemical weathering, whereas surface water flow is the principal erosive agent.

4. Methodology

The three Sierra Norte peneplain levels were taken as reference points around which weathering profiles were intensely sought. The areas close to the dacitic stock (Fig. 1) were not taken into account to avoid superposition of the hydrothermal and weathering processes. Two profiles in road construction land cuts were selected with the following stringent criteria: They should be similar to the parent rock in texture and have a favorable geomorphic setting (Middelburg et al., 1988).

These profiles are located at different topographic heights, and in both cases, the visible thickness is approximately 2 m. Different horizons were defined within each profile on the basis of macroscopic characteristics (Figs. 2 and 3) such as coloring, compaction, texture, and mineralogy; four levels were found in one profile and five in the other, and 2-3 Kg samples were taken from each after cleaning the exposed surface with a spade.

Thin sections from the protolith and lower horizons were prepared in samples from La Quinta profile. Samples from the Tulumba profile were unsuitable for thin section preparation. Chemical analyses and identification of the clay mineralogy from each horizon were performed using a combination of refraction microscopy, granulometric analysis, X-ray diffraction (XRD), and scanning electron microscopy.

The XRD patterns were obtained at CIMAR, Universidad Nacional del Comahue, using CuKα radiation with a Rigaku DII-Max diffractometer, horizontal goniometer, Ni-filter, scan 2° θ/min, 0.05° 2θ step, and running 2° and 40° 2θ. Samples were crushed, then ultrasonically dispersed in water, and the <2 μm fraction was separated by centrifugation (Brindley and Brown, 1980). Slides were air dried, ethylene glycol solvated, and, after having been heated to 375 °C for 1 hr and to 550 °C for 2 hrs, Mg saturated, dispersed, and pipetted onto glass slides to make oriented aggregates. The clay minerals were identified according to Moore and Reynolds (1997).

The geochemical analyses were performed at Acme Analytical Laboratories S.A., Santiago de Chile. Major and certain trace elements (Ba, Ni, Sr, Zr, Y, Nb, Sc) were discerned in chips by X-ray fluorescence spectrometry on fused discs (0.200 g samples were fused with 1.2 g of $LiBO_2$ and dissolved in 100 ml 5% HNO_3). Other trace elements and rare earth elements (REE) were discerned in pulps by ICP/MS by $LiBO_2$ fusion.

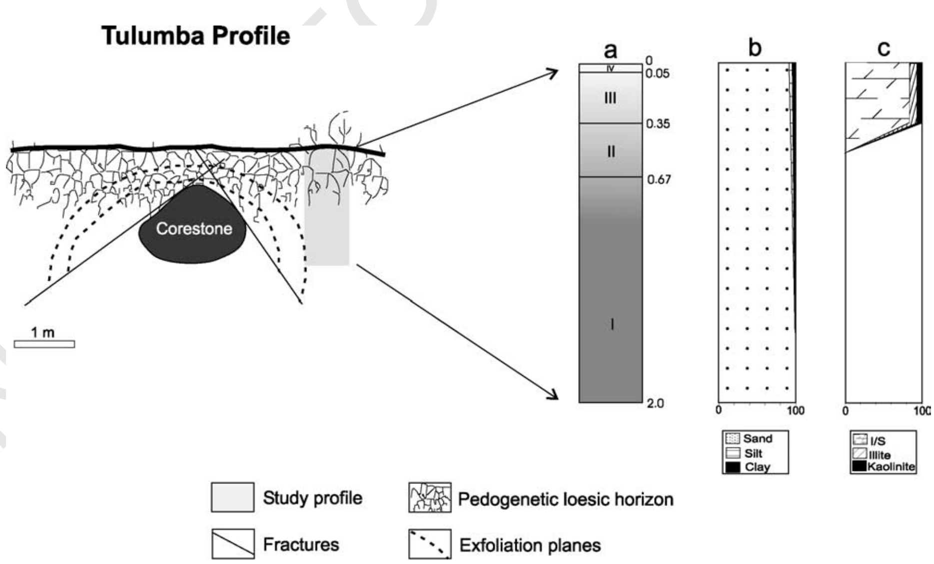

Fig. 2. Tulumba profile. (a) Cross-section details; (b) grain size fraction (the lack of primary cohesion made it possible to carry out a granulometric study from the base of the profile); (c) clay mineral percentages. A corestone was taken as the parent rock.

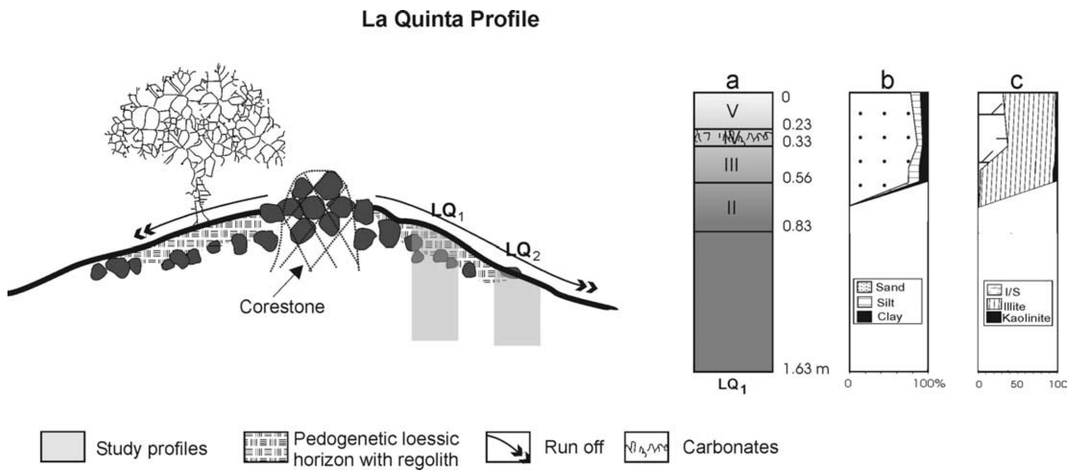

Fig. 3. La Quinta profile.(a) LQ_1 cross-section details; (b) grain size fraction; and (c) clay mineral percentages. A corestone was taken as the parent rock.

5. Results

5.1. Tulumba profile

This profile is located at the intersection of the road from Dean Funes to Tulumba and the road to San Pedro Norte (S30°24'24", W64°13'18"). It evolves on porphyritic granite with large euhedral microcline phenocrysts pertaining to the Tulumba porphyritic granite unit (Baldo et al., 1998). Four horizons were defined over a thickness of 2 m; the protolith sample was taken from a corestone near the profile (Fig. 2).

5.1.1. Macroscopic characteristics of the weathered rock

Level I (2.0–0.67 m) was defined as incipiently weathered rock that breaks into greater than 5 cm blocks. Level II (0.67–0.35 m) is reddish in color and crumbles easily to a fine gravel texture. In level III (0.35–0.05 m), the altered granite is mixed with silty sediments with blocky soil structures, whereas level IV represents a 5 cm thick horizon, rich in organic matter with well-differentiated pedogenic characteristics. Altered and broken-down biotite, which is the most abundant ferromagnesian mineral, accounts for the red coloration. There is an increase in the percentage of silt and clay particles in the uppermost layers (Fig. 2b), indicating a coherent evolution with respect to profile development (Gouveia et al., 1993; Condie et al., 1995).

5.1.2. Petrographic characteristics of the protolith or parent rock

This sample is a coarse-grained, porphyric monzogranite; the essential minerals are quartz, microcline, plagioclase, and biotite. Muscovite, zircon, apatite, and opaque phases occur as accessory minerals; chlorite, sericite, clay phases, rutile, and other unidentified iron oxides are present as secondary minerals. Microcline phenocrysts are euhedral, and the small crystals are anhedral; the phenocrysts are perthitic and display a poikilitic texture enclosing small euhedral crystals of plagioclase, quartz muscovite, and biotite. Sericite and clay alteration is incipient and occurs in patch form. Plagioclase (oligoclase) is euhedral to subhedral and contains incipient sericite and clay alteration. Subhedral biotite 'books' contain chlorite along their borders, penetrating inward along the cleavage planes; iron-depleted aggregates associated with rutile are also clearly visible. Pristine muscovite is scarce and always associated with biotite. Euhedral zircon and apatite crystals occur as inclusions in biotite and feldspar minerals.

The degree of alteration in the weathered levels made it impossible to prepare thin sections for petrographic studies.

5.2. La Quinta profile

This profile is located close to Arroyo la Quinta on the secondary road that leads toward Villa María de Río Seco from the road between San Francisco del Chañar and Rayo Cortado (S29°54'38", W63°53'00"). It is visible in the cutting of a road through a gentle hill. The profile evolves on a coarse-grained porphyritic granite similar to Tulumba granite, in which the transition from granite to weathered rock is also visible. The observable thickness of the five layers noted reaches 1.63 m (Fig. 3). The parent rock sample was obtained from a corestone. The presence of some disturbance factors in the profile (e.g., a pedogenetic horizon with regolith, runoff effects) led us to make a duplicate sample at 8 m distance to check the information. Analyses in both profiles showed similar results.

5.2.1. Macroscopic characteristics of the weathered rock

Level I is characterized by intense fracturing, with the formation of large blocks. Level II is distinct from level I by the occurrence of comparatively smaller block sizes and a reddish color. Level III presents a fine gravel texture, in

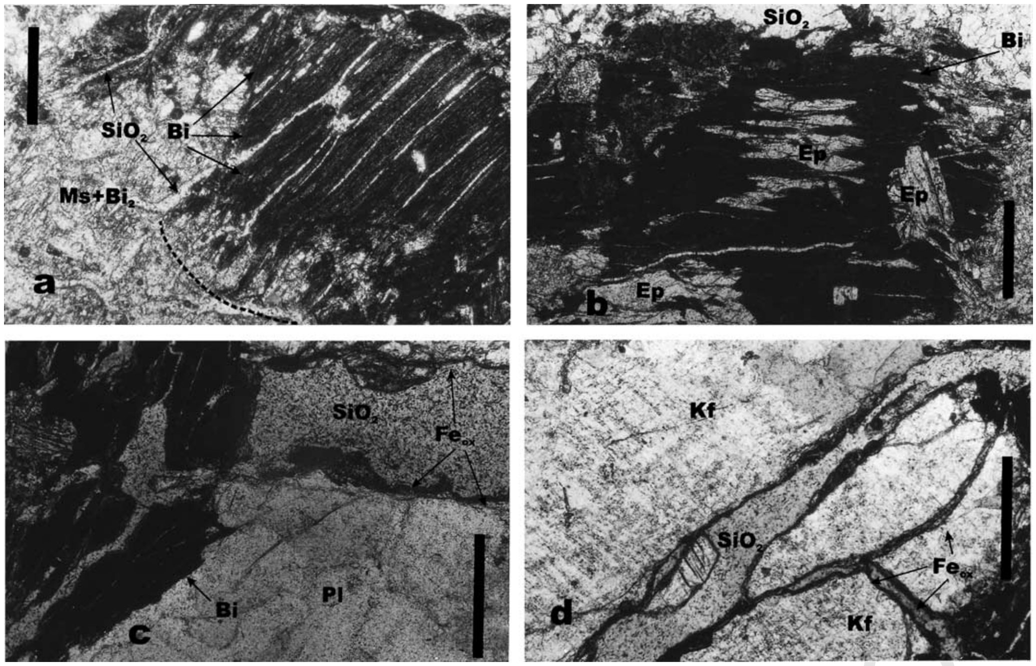

Fig. 4. (a-b) Photomicrographs of hydrothermal processes in La Quinta parent rock. (a) Fractured biotite with microcrystalline quartz veins, open cleavages, and a muscovite + neobiotite mass. Parallel polarizers. (b) Fractured biotite with microcrystalline quartz veins, transformed to muscovite, neobiotite, and epidote. Crossed polarizers. (c-d)Weathering processes in LQ_1 level II. (c) Transcrystalline fracture with silica filling and Fe-oxides across an argillized crystal of plagioclase and an opened biotite. Parallel polarizers. (d) Argillized K-feldspar with transcrystalline fracture filled by silica and Fe-oxides. Crossed polarizers. Bi, biotite; Bi_2, neobiotite; Ms, muscovite; SiO_2, microcrystalline quartz; Ep, epidote; Pl, plagioclase; Fe_{ox}, Fe oxides; Kf, K-feldspar. The bar represents 1 mm.

which clasts up to 2 cm are rare and roots are abundant. Levels IV and V consist of loess-like sediments with abundant regolith fragments, but level IV differs in its high carbonate content.

5.2.2. Petrographic characteristics of the parent rock

A medium-grained, porphyritic monzogranite, it shows ductile deformation and signs of hydrothermal activity. It is composed of quartz, plagioclase, microperthitic potassium-feldspar, and biotite as essential minerals; muscovite, apatite, zircon, and opaques as accessory minerals; and chlorite, epidote, phyllosilicates, Fe-Ti oxides, and microcrystalline quartz are secondary products. Two types of quartz were identified: One is of medium grain size, consertal texture, and undulate extinction, whereas the other is of fine grain size and mosaic texture, indicating deformation and recrystallization processes. The second type is interstitial and appears in fissures and on the plagioclase borders in coronitic arrangement. Large zoned and multiply twinned plagioclase grains are selectively altered to sericite in the nucleus of the zoned crystals, along the cleavage planes, and as patches, and they present pervasive argillization. The potassium feldspar is anhedral microperthitic orthoclase with incipient muscovite and clay alteration. Flexured biotite has a dark greenish brown color with dark brown Fe-oxides marking the cleavage traces; it also shows corroded borders associated with recrystallization and new growth of microcrystalline quartz, muscovite, and Fe-Ti oxides. Smaller biotite crystals, suggesting a second generation, can also be seen in cleavage planes. Biotite and feldspar grains contain tiny euhedral zircon and apatite inclusions without any evidence of alteration.

5.2.3. Petrographic characteristics of the weathered rock

The following observations are based on a petrographic analysis of the distinct weathered horizons. The lack of cohesion of the weathered levels in the Tulumba profile made it impossible to prepare thin sections of that site, so petrographic analysis was not carried out there. Consertal quartz crystals show the greatest resistance to weathering and remain grouped; in contrast, the microcrystalline variety disintegrates and lodges in fractures. Clay and sericite alteration of plagioclase increases toward the surface levels in the profile, whereas microcline crystals show no changes along the profiles (LQ_1 and LQ_2). Biotite is the mineral most altered during weathering (Fig. 4a and b). Iron leaching is the most common process acting on biotite in the profiles analyzed. Biotite in the protolith has a dark, greenish brown color with dark brown Fe-oxides marking the cleavage traces. In profile LQ_1, this mineral changes color and pleochroism as a consequence of weathering, varying from bright yellow brown to intense red as a result of Fe-oxide liberation that masks the anisotropic colors. In profile LQ_2, biotite crystals are similar

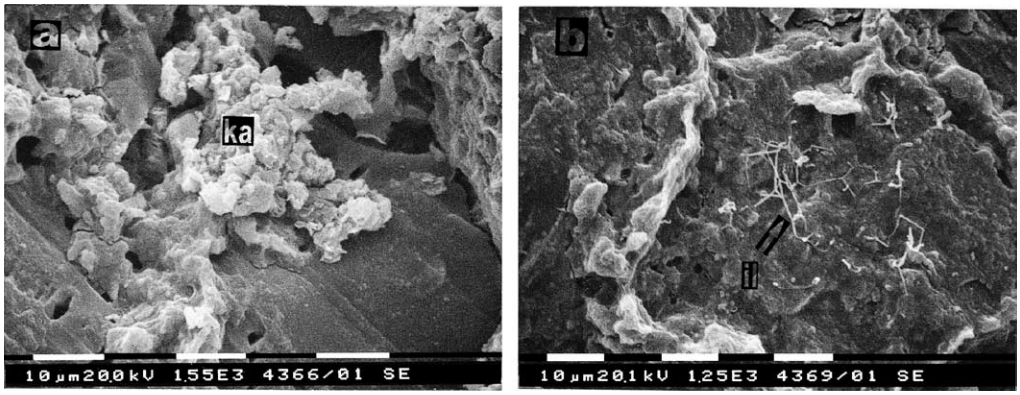

Fig. 5. (a) Neoformed kaolinite associated with feldspars. (b) Neoformed illite associated with mica. La Quinta profile. Ka, Kaolinite; Il, Illite.

to those in profile LQ_1, but the Fe-oxides are concentrated in pits and the sheets are highly kinked.

When the physical effects of weathering are analyzed in both profiles, an increase in the density and thickness of fractures is noted as the profile evolves from bottom to top. Fracture thickness varies between 0.15 and 0.7 mm, and fracturing density increases gradually. Fine fractures without displacement arise bordering the feldspar phenocryst, availing of the cleavage in biotite. Other fractures are transcrystalline and cross the surface of the rock in all directions.

In both LQ profiles, fractures are filled with a microcrystalline phyllosilicate, and there is a similar change in the rock structure along the depths. In levels II and III, increasing microfracturing of the minerals in contact with the fissures leads to displaced fragments cemented by clay material; these characteristics give the rock a micro-breccia texture.

6. Clay mineralogy

A semiquantitative estimation of clay mineral proportions was performed in the upper levels (III and IV) of both profiles. In Tulumba profile, samples show similar values, with illite being the dominant phase (93%) and subordinate quantities of interstratified illite/smectite (I/S) type R0 (6%) and kaolinite + chlorite (1%).

In La Quinta profile, the clay mineralogy studies in the upper levels indicate a predominance of illite in level III (93%) (Fig. 5b), which decreases to 60% in level IV, with a significant increase in interstratified I/S type R0 (35–39%). Originally scarce kaolinite + chlorite pass from 5% content in level III to 2% content in level IV.

Illite is the most abundant clay mineral in both profiles, followed by interstratified I/S type R0. Kaolinite + chlorite are the least common (5-1%). Scanning electron microscope observations show that they are principally of an inherited type (illite and I/S), as they are morphologically irregular. Neoformed illite over micas and neoformed kaolinite over feldspars are also present in subordinate quantities.

There is a noticeable increase of illite along the depth in La Quinta profile (Fig. 3). Illite in ribbon-like forms appears on the micas and feldspars, suggesting that its genesis is related to mineral alteration. Interstratified I/S of type R0 have irregular flake-like forms and are found mainly as detritics. We also found I/S in smaller amounts in association with mica, which suggests an origin in the alteration of this mineral. The alteration of biotite to I/S species liberates iron oxides and hydroxides that accumulate in the zones of maximum aeration; in the profiles studied, these correspond to inter- and transcrystalline fracture surfaces (Fig. 4c and d). Kaolinite occurs as crystals of less than 0.5 µm and is associated with potassium feldspar and plagioclase (Fig. 5a).

Chlorite development results from the gradual alteration of biotite and forms in crystalline defects and on inclusions, as well as by iron oxidation at the junction of the phyllosilicate sheets. These actions generate microdivisions within the mineral, reducing its size, and as a consequence, the process at the sheet junctions accelerates the liberation of cations (Millot, 1964). In the case of biotite, Fe, Ti, and Mg ions occupy the intermediate sites producing chlorite alteration of biotite with an exsolution of iron oxides, as observed in petrographic sections.

7. Geochemistry

Chemical analyses were performed on each of the levels in the profiles studied (Tulumba, LQ_1, and LQ_2); the concentration of major and trace elements present in profile samples is shown in Table 1.

The chemical alteration index (CIA), which results in a quantitative weathering parameter (Nesbitt and Young, 1997), was calculated on the basis of the data presented in Table 1 as follows:

$$CIA = 100 \times [Al_2O_3/(Al_2O_3 + CaO + Na_2O + K_2O)]. \tag{1}$$

Table 1
Geochemical analysis of weathering profiles of Sierra Norte, Córdoba.

Sample	T-RM	T-I	T-II	T-III	T-IV	LQ-RM	LQ-I	LQ-II	LQ-III	LQ-IV	**LQ-V**	**LQ-Ib**	**LQ-IIb**	**LQ-IIIb**	**LQ-IVb**	**LQ-Vb**
Major elements (wt. %)																
SiO_2	67.35	64.68	65.10	67.73	65.30	68.77	69.61	70.39	73.60	66.53	68.18	71.88	69.73	72.60	71.21	68.73
Al_2O_3	15.53	14.90	15.42	14.35	14.25	14.67	14.40	13.93	13.59	13.11	13.79	13.73	14.47	13.41	14.00	13.72
Fe_2O_3	4.60	6.49	5.86	4.90	5.32	4.93	4.05	3.68	2.05	3.01	3.82	3.05	4.16	2.45	2.89	3.91
MgO	1.17	1.71	1.55	1.19	1.32	1.31	0.78	0.66	0.34	0.59	0.75	0.53	0.69	0.44	0.53	0.73
CaO	1.79	2.31	2.06	1.71	1.90	2.08	1.53	1.41	1.14	4.31	2.08	0.37	0.88	0.83	1.46	1.55
Na_2O	2.80	2.55	2.41	2.10	2.03	2.50	2.48	2.44	2.37	2.41	2.43	2.82	2.54	2.47	2.62	2.50
K_2O	4.73	3.30	3.89	4.04	3.27	4.49	4.58	4.74	4.47	4.80	4.59	5.34	4.52	4.95	5.08	4.24
TiO_2	0.66	0.95	0.86	0.67	0.75	0.67	0.57	0.50	0.27	0.41	0.55	0.40	0.56	0.33	0.38	0.54
P_2O_5	0.24	0.26	0.25	0.20	0.29	0.18	0.22	0.18	0.11	0.15	0.21	0.15	0.17	0.13	0.15	0.19
MnO	0.08	0.10	0.10	0.07	0.08	0.09	0.06	0.06	0.04	0.05	0.06	0.04	0.06	0.04	0.04	0.06
LOI	0.80	2.50	2.20	2.80	5.20	0.81	1.50	1.80	1.80	4.40	3.30	1.40	2.00	2.10	1.40	3.60
SUM	100.00	99.93	99.91	99.98	99.93	100.49	99.97	99.97	99.97	99.95	99.96	99.90	99.96	99.97	99.95	99.96
CIA	54.48	55.46	56.40	56.75	58.18	54.10	54.93	54.34	55.70	49.95	51.97	55.32	57.56	55.10	52.91	54.36
Trace elements (ppm)																
Ba	934	379	571	603	394	747	559	537	635	530	488	620	510	573	593	473
Ni	26	34	38	41	29	–20	20	20	20	23	31	31	25	20	20	32
Sr	145	120	130	119	107	133	114	109	112	112	108	91	105	104	113	107
Zr	191	299	312	233	278	261	194	166	114	141	215	136	178	145	121	176
Y	31	58	59	41	49	33	55	52	28	41	47	32	37	27	32	42
Nb	10	10	10	10	10	18	10	10	10	10	10	10	10	10	10	10
Sc	2	3	3	2	2	11	2	2	1	1	2	1	2	1	1	2
Co	10	15	13	11	12	9	8	7	4	6	8	5	8	6	5	7
Cs	14	21	19	14	17	12	9	7	7	7	8	7	7	7	7	9
Ga	18	20	21	16	18	19	17	16	13	15	16	13	17	13	15	16
Hf	6	10	9	7	9	7	7	6	4	5	7	4	8	4	5	7
Nb	21	36	31	24	26	18	21	18	9	16	21	10	22	10	14	20
Rb	238	238	240	197	193	193	221	203	191	210	211	198	228	198	204	196
Sn	7	11	8	6	7	3	7	7	4	6	8	5	9	5	7	8
Sr	136	117	126	110	106	133	109	100	107	109	101	98	102	98	108	102
Ta	1	2	2	2	2	2	2	1	1	1	2	1	2	1	1	2
Th	15	25	21	16	22	20	19	17	11	15	20	12	20	12	14	19
Tl	1	1	1	1	1	1	1	1	1	1	1	1	1	1	1	1
U	2	4	4	3	4	3	2	3	2	2	3	2	4	2	2	3
V	73	104	104	74	88	75	69	68	40	44	61	39	78	39	54	53
W	3	4	4	9	8	2	2	3	2	2	5	6	7	6	3	7
Zr	232	402	328	280	363	264	237	207	156	174	254	150	269	150	197	223
Y	35	65	67	42	55	33	58	55	36	37	52	30	43	30	39	50
Rare earth elements (ppm)																
La	42.1	63.4	56.3	50.3	56.2	49.3	43.7	42.8	27.7	36.6	45.6	30.8	49.2	25.3	34.1	40.7
Ce	86.8	125.3	112.8	94.9	121.1	102.0	88.3	81.0	55.3	70.9	90.3	65.9	92.2	60.2	68.0	86.4
Pr	11.5	17.8	16.2	13.5	15.8	9.7	12.4	11.7	7.5	9.5	12.2	8.6	13.4	7.1	9.4	11.6
Nd	45.8	73.1	65.4	56.3	63.3	42.6	49.9	46.6	28.9	39.6	50.0	34.7	54.2	27.7	35.6	45.4
Sm	8.9	14.4	13.9	10.7	12.8	8.2	9.9	7.0	9.5	10.8	5.7	5.7	7.7	7.2	9.8	9.4
Eu	1.7	2.0	2.1	1.7	1.5	1.5	1.4	1.2	1.4	1.5	1.2	1.0	1.2	1.4	1.3	1.3
Gd	7.8	13.3	12.0	9.9	11.1	6.8	9.2	6.2	8.8	3.4	5.3	4.9	7.1	6.4	8.6	8.0

Tb	1.2	1.9	1.9	1.4	1.7	1.1	1.6	1.1	1.6	1.4	1.0	0.9	1.2	1.2	1.6	1.5
Dy	6.7	11.3	11.0	7.5	9.6	6.0	9.7	6.0	9.5	7.7	6.0	5.2	6.7	6.9	9.0	8.7
Ho	1.1	2.1	2.0	1.4	1.7	1.2	1.8	1.0	1.8	1.3	1.2	0.9	1.2	1.2	1.7	1.5
Er	3.7	6.8	6.8	4.2	5.9	3.6	5.9	3.4	5.9	4.2	3.9	3.1	3.9	4.1	5.7	5.3
Tm	0.5	1.0	1.0	0.6	0.8	0.6	0.8	0.5	0.8	0.6	0.5	0.4	0.5	0.6	0.8	0.7
Yb	3.4	6.5	6.3	4.0	5.7	3.5	5.4	3.0	5.3	4.1	3.5	2.8	3.6	3.5	5.0	4.7
Lu	0.4	0.8	0.8	0.5	0.7	0.5	0.6	0.4	0.7	0.5	0.4	0.4	0.4	0.4	0.6	0.6

Trace elements and REE determined by ICP/MS in ACME ANALYTICAL LABORATORIES S.A., Santiago de Chile. Notes: Major elements determined by x-ray fluorescence spectrometry on fused discs.

We expect high CIA values, concordant with the maturity of geoforms. However, the range of CIA values for both profiles lies within the values corresponding to incipient weathering (<60). The values define an increasing trend toward the upper levels of each profile. An estimate of "chemical behavior" during weathering can be obtained from the relationship between the elemental concentration in weathered rock and the corresponding concentration in unaltered or less altered rock, which is here referred to as the protolith or parent rock (Figs. 6 and 7,). Mass relations between the protolith and the weathered products are determined by gains or losses, produced as a result of the hydrolysis of certain minerals and the precipitation of others. One solution to this problem is to define the relationship between the different elements and a single element considered immobile, because it should not have suffered changes in its concentration during protolith weathering. According to Nesbitt (1979); Nesbitt and Markovics (1997), the percentage change is established as follows:

$$\%\ \text{change} = 100 \times [(X^m/I^m)/(X^p/I^p)] - 1, \qquad (2)$$

where:

X^m is the concentration of an element in the sample,

I^m is the concentration of the immobile element in the sample,

X^p is the concentration of the element in the protolith, and

I^p is the concentration of the immobile element in the protolith.

We assume that (1) the weathered material comes from the protolith and (2) at least one element remains immobile during weathering. In this case, aluminum is considered immobile. The results of profiles LQ_1 and LQ_2 were plotted together to determine whether the results obtained were similar in each.

The percentage change in major elements from the Tulumba profile is plotted in Fig. 6a. The positive values indicate enrichment, whereas negatives correspond to losses with respect to the protolith. Na_2O depletion is observed throughout the profile, and Fe_2O_3, MgO, CaO, TiO_2, and MnO show the same tendency, with an accumulation level close to the protolith.

It should be noted that protolith plagioclase shows evidence of sericite and clay alteration prior to weathering, which makes it the least stable mineral that displays an increase in these processes as the profile evolves. The minor elements (Fig. 6b and c) show significant losses in Ba; there is a constant loss of Sr along the profile, but Rb losses appear only in the uppermost levels (III and IV). Zr, Y, and Cs show a similar tendency, with enrichment along the profile, especially in levels I and II. Nb, Sn, Th, and V show enrichment along the profile, especially in level I.

In La Quinta, covariation between both profiles (LQ_1 and LQ_2) is observed with the depletion of major elements

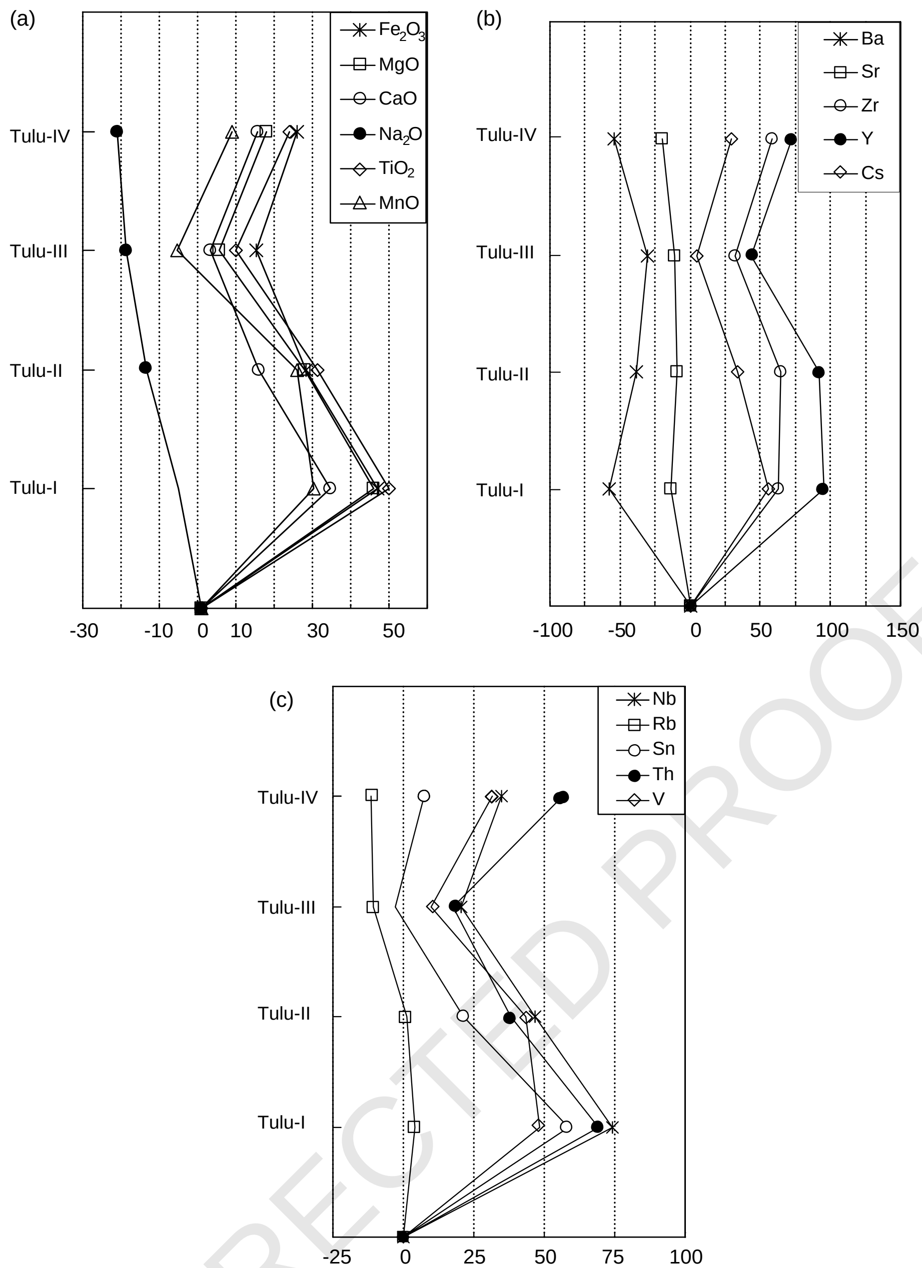

Fig. 6. Percentage of change of major trace elements relative to the "immobile" species Al_2O_3 (Nesbitt, 1979), Tulumba profile. The abscissa is given by equation (2), and the ordinate shows the sample order in the profile. (a) major elements, (b-c) trace elements.

(Fig. 7a and b). Trace elements (Fig. 7c and d) also suffer depletions, except for Y and Sn, which increase in the profile.

The REE values normalized to parent rock (Fig. 8) show a general enrichment along the Tulumba profile, with the highest values in levels I and II. Europium is the only element impoverished in the upper levels. The La Quinta profile shows a different trend, with enrichment in HREE and impoverishment in LREE, particularly La and Ce. The lower levels (LQ I and II) are enriched in REE, with the exception of La and Ce. Level III corresponds to a leaching zone and shows the lowest concentrations of light lanthanides in particular.

8. Discussion

The profiles studied have similar parent rocks, which were subjected to hydrothermal processes of varying intensity. These processes were much more intense in the La Quinta area and are mineralogically expressed in plagioclase sericitization and argillization, biotite chloritization, crystallization of a smaller neobiotite, and quartz recrystallization. We relate these observations to the hydrothermal alteration system associated with the dacite-rhyolite intrusion (Lira et al., 1995) (Fig. 1), which affected not only the rocks immediately surrounding the stock but also areas such as La Quinta, more than 25 km away.

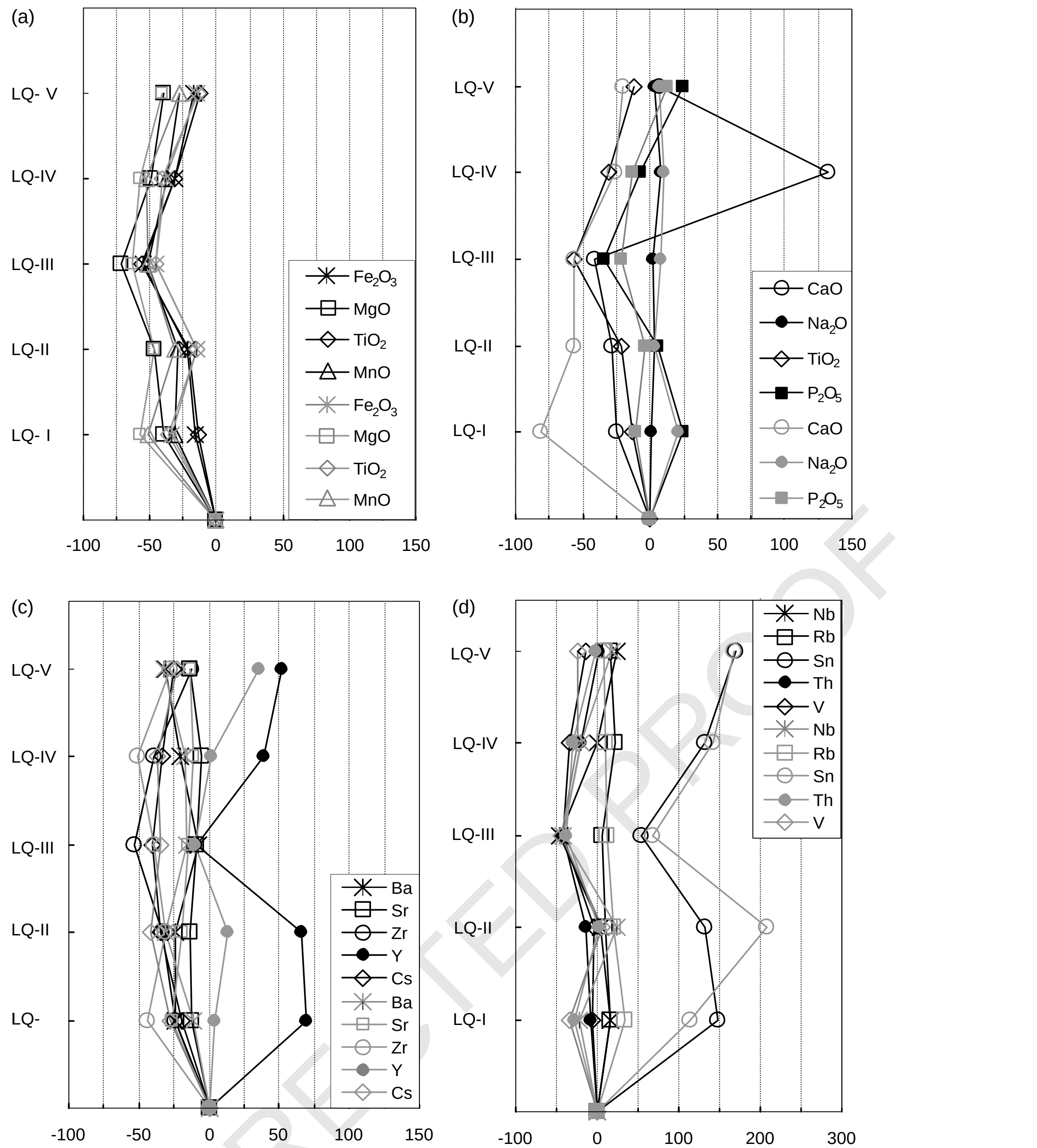

Fig. 7. Percentage of change of major and trace elements relative to the "immobile" species Al_2O_3 (Nesbitt, 1979), La Quinta profile. LQ_1 values in black and LQ_2 values in gray. The abscissa is given by equation (2), and the ordinate shows the sample order in the profile. (a-b) major elements, (c-d) trace elements.

Greater cohesion in La Quinta permitted the preparation of thin sections along the profile, which made it possible to observe the microscopic characteristics of weathered levels. An increase in the density and thickness of fractures is noted from bottom to top; these fractures are filled by a microcrystalline phyllosilicate with Fe oxides followed by microcrystalline quartz (Fig. 8d).

Clay minerals are dominantly illite species. They are generally of an inherited type and, to a lesser extent, neoformed. Enrichment in I/S species in the La Quinta profile probably indicates the action of pedogenic processes (Thieboult et al., 1989). The scarce neoformed clay minerals originate in micas and feldspars (illite), micas (I/S), biotite (I/S and chlorite), and K-feldspar and plagioclase (kaolinite).

Three distinct horizons are broadly discernible in the profiles studied: leaching processes are dominant in one, accumulation in another (clay eluviation, carbonate alteration, and red coloration), and fragmentation and fracturing closer to the protolith in the third. Throughout Tulumba profile, the observed Na_2O loss may be due to incongruent dissolution of plagioclase (Van der Weijden and van der Weijden, 1995), consistent with the maximum solubility of Na that, once in solution, can migrate away from the profile.

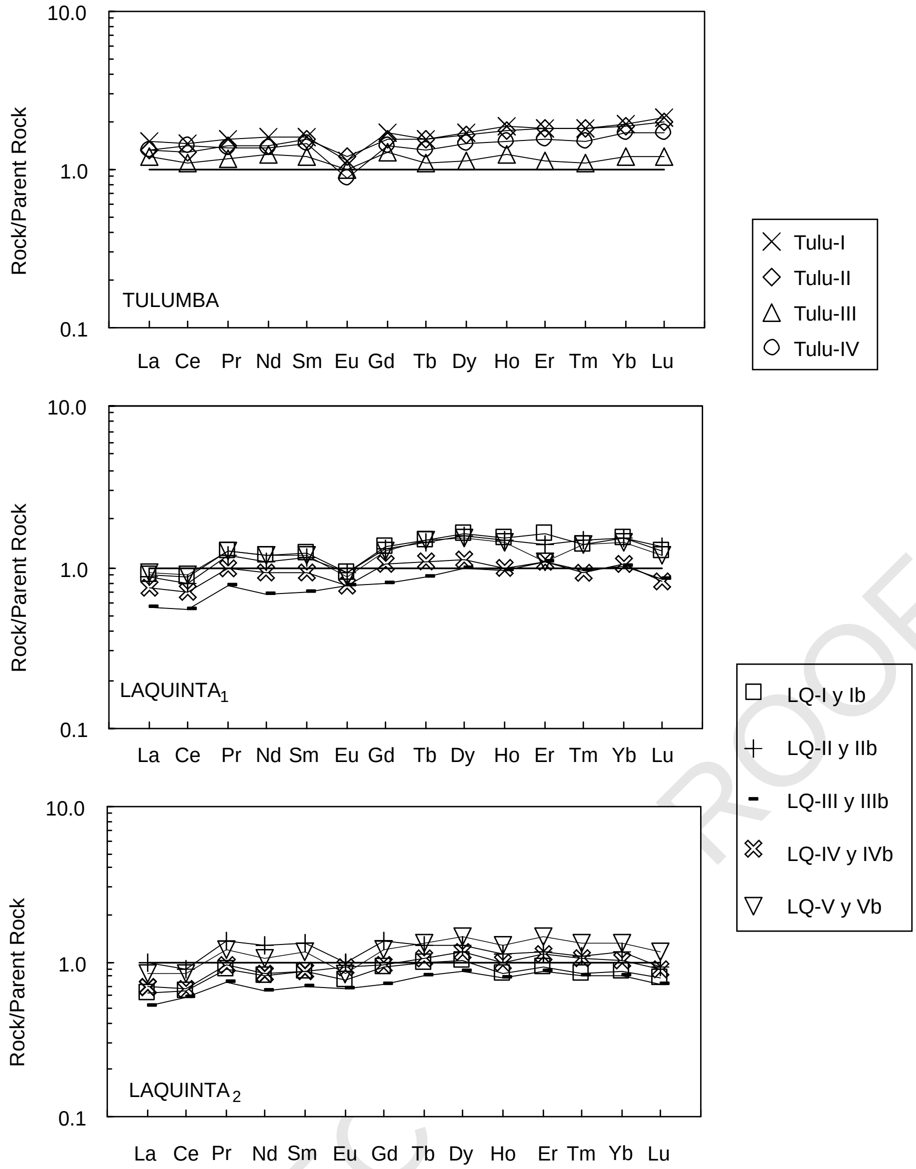

Fig. 8. Rare earth elements normalized to a corestone (parent rock.). (See explanation in text.)

We interpret the enrichment in MgO, TiO_2, MnO, and CaO observed in Tulumba profile as a phenomenon associated with the precipitation of secondary oxides and calcite in fractures. The minor elements (Fig. 6b and c) show losses in Ba, Sr, and Rb; Ba replaces K in the biotite structure, Rb enters the crystalline structure of K-feldspar and biotite, and Sr enters both feldspars, indicating that biotite is the mineral most readily altered during weathering. The enrichment in Zr, Y, Sn, Th, and V is interpreted as due to the higher concentration of accessory minerals relative to the original granite because they are resistant to weathering. Enrichment of these elements in soil is attributed to pedogenic processes.

In the La Quinta profiles (LQ_1 and LQ_2), the depletion of major elements (Fig. 7a and b) is attributed to the alteration of biotite and opaque minerals, with subsequent hydrolysis and migration of Fe, Ti, and Mn. In the case of Fe, it is known that only Fe^{2+} is soluble and can migrate. It is likely that organic materials promote the reduction and leaching of iron. The anomalous CaO value in LQ IV (Fig. 7b) is associated with a nonuniform, carbonate-rich level and related to the pedogenic processes mentioned previously, specifically carbonate alteration. The high increase in Y and Sn may be explained by the random presence of apatite and opaques in the granite. A source for these minerals may also be loess-type sediments present in the superficial levels of the profile.

The REE patterns in the Tulumba profile (Fig. 8a) show REE enrichment in the deepest levels as a result of leaching processes in the uppermost horizons, transport in solution, and final precipitation of REE near the protolith. The impoverishment in Eu in the uppermost levels results from the weathering of feldspars; Middelburg et al. (1988) point out that in contrast to other REE, Eu as Eu^{2+} is preferentially incorporated in feldspar during magmatic processes and thus easily liberated in weathering processes due to its susceptibility to alteration.

In the La Quinta profile, REE patterns different than those of Tulumba might be caused by non-homogeneities in the parent rock (Van der Weijden and van der Weijden, 1995) and/or differences in the susceptibility to weathering of the protolith minerals. Bearing in mind this last criterion, the effects of a hydrothermal front affecting the La Quinta profile must be considered, which may have produced percolating solutions under different pH-Eh conditions.

Redox transformations are important in the determination of element mobility. The geochemical behavior of Mn, Cr, V, Fe, and Ce is very dependent on the redox state of a weathering system. These redox transformations can be useful to set limits on the oxidation state of a weathering suite (Middelburg et al., 1988). In the La Quinta profile losses in Fe, Mn, V, and Ce (Figs. 7a and 7d, 8b and c) point to local reduction conditions that permitted the migration of Fe^{2+} out of the profile, accompanied by the other redox-sensitive elements.

Herrero (2000), who identifies three topographic highs located at different levels and separated by abrupt escarpments, decrypted the geomorphological features of the Sierra Norte. The hills have similar heights, with flat tops and generally convex slopes, domed hills, corestone or boulder tors, inselbergs, and silcretes with polygonal cracks. These features indicate a landscape that resulted from a long weathering history. The apparent incompatibility between the maturity of the landscape and the geochemical signature can be explained by the probable removal, through erosion, of the most weathered horizons in the profiles. These horizons were associated with ancient peneplains, which are only preserved as occasional geomorphological relicts.

The study of landscape evolution is made easier by the terrestrial *in situ* cosmogenic nuclide method. Single or multiple nuclides (^{3}He, ^{10}Be, ^{14}C, ^{21}Ne, ^{26}Al, and ^{36}Cl) can be measured in a single rock surface to obtain erosion rates on boulder and bedrock surfaces for exposures ranging from 10^2 to 10^7 years (Gosse and Phillips, 2001). Such studies should be initiated in Sierra Norte to determine the time of exposure of peneplained surfaces to cosmic radiation, which will make it possible to date the periods in which the weathering processes occurred.

9. Conclusions

The profiles studied are poorly developed, as indicated by the absence of saprolithic levels, the predominance of the sand fraction in the granulometric analysis of the weathered levels with low clay contents (Figs. 2b and 3b), and CIA values <60. Clay minerals are dominantly illite species, which are generally of an inherited type and, to a lesser extent, neoformed.

The Tulumba profile is developed on porphyritic biotite granite, in which four weathering levels were discerned. The red coloration is ubiquitous and results from the weathering of biotite that liberates iron oxides and hydroxides deposited in the fractures. The clay minerals are predominantly illites, with a lesser quantity of type R0 interstratified I/S; kaolinite and chlorite are scarce and result from the weathering of feldspars and biotite, respectively.

The La Quinta profile is developed on coarse-grained porphyritic granite, in which five layers can be discerned. Petrographic observation reveals the overprint of weathering alteration on hydrothermal processes, the latter of which are expressed in plagioclase sericitization, argillization and epidotization, biotite chloritization, crystallization of a smaller neobiotite, and quartz recrystallization. The clay minerals of level III are illitic; the significant increase in I/S in level IV is attributed to pedogenic processes. Kaolinite and chlorite are less common, and their combined volume percentage varies between 5% in level III and 2% in level IV. Moreover, the granulometric evolution of the profile is not linear, as a result of the presence of regolithic material in the upper levels, derived from stream run-off.

Increases and decreases in the REE contents, as well as differences in the REE patterns, can by caused by differences in the susceptibility to weathering of the protolith minerals after hydrothermal conditions. The REE patterns in the Tulumba profile (Fig. 8a) show an enrichment in REE in the deepest levels, the result of leaching processes in the uppermost horizons, transport in solution, and final precipitation of REE near the protolith. The impoverishment in Eu in the uppermost levels may be a result of the weathering of feldspars. In the La Quinta profile, losses of Fe, Mn, V, and Ce (Figs. 7a and d, 8b and c) point to local reduction conditions, which permitted the migration of Fe^{2+} out of the profile, accompanied by the other redox-sensitive elements.

Common features in the mineralogical, petrographic, and geochemical information indicate incipient weathering. In addition, all the regions studied are associated with relict landscapes. The apparent incompatibility between the maturity of the landscape and the geochemical signature can be explained by the probable removal, by erosion, of the most weathered horizons in the profiles. These horizons are associated with ancient peneplains, which are only preserved as occasional geomorphological relicts.

To attain a correct paleoenvironmental interpretation of the region, it will be necessary to advance the reconstruction of these ancient surfaces while dating the exposure of the peneplained surfaces through cosmogenic isotope analysis, which will make it possible to set time boundaries on the weathering processes studied.

Acknowledgements

Dr Eduardo Piovano is thanked for his help in the field and constructive discussions. Dr Mónica López de Luchi and an anonymous reviewer contributed observations that permitted a significant improvement of this work. The Consejo de Investigaciones of the Universidad Nacional of Salta (Proyect 982) and the Agencia Nacional de Promoción Científica y Tecnológica (A.N.P.C.yT.) PICT 07-00000 and PICT 07-08524 financed this work.

References

Baldo, E.G., Pankhurst, R.J., Rapela, C.W., Saavedra, J., Mazieri, C., 1998. Granito ‘El Cerro’, magmatismo colisional famatianiano en el sector austral de la Sierra Norte-Ambargasta, Córdoba. X Congreso Latinoamericano de Geología y VI Congreso Nacional de Geología Económica, Actas II, 374–378.

Brindley, G., Brown, G., 1980. Crystal Structures of Clay Minerals and their X-ray Identification. Mineralogical Society, London p. 495.

Caminos, R., 1979. Sierras Pampeanas Noroccidentales. Salta, Tucumán, Catamarca, La Rioja y San Juan. In: Segundo Simposio de Geología Regional Argentina 1, Academia Nacional de Ciencias, Córdoba, pp. 225–291.

Castellote, P., 1985. Algunas observaciones geológicas en la Sierra de Ambargasta y Sumampa. Acta Geológica Lilloana 16 (2), 259–269 (Provincia de Santiago del Estero).

Cioccale, M., 1999. Investigación geomorfológica de cuencas serranas. Estudio geomorfológico integral: morfodinámica, morfometría y morfogénesis del flanco oriental de las Sierras Chicas de Córdoba. Tesis doctoral, Facultad de Ciencias Exactas, Físicas y Naturales, Universidad Nacional de Córdoba, p. 121. Unpublished.

Condie, K.C., Dengate, J., Cullers, R.L., 1995. Behavoir of rare earth elements in a paleoweathering profile on granodiorite in the Front Range, Colorado, USA. Geochimica et Cosmochimica Acta 59 (2), pp. 279–294.

Gosse, J.C., Phillips, F.M., 2001. Terrestrial in situ cosmogenic nuclides: theory and application. Quaternary Science Reviews 20, 1475–2560.

Gouveia, M.A., Prudêncio, M.I., Figueiredo, M.O., Pereira, L.C.J., Waerenborgh, J.C., Morgado, I., Pena, T., Lopes, A., 1993. Behavoir of REE and other trace and major elements during weathering of granitic rocks, Évora, Portugal. Chemical Geology 107, 293–296.

Herrero, S.A., 2000. Procesos sedimentarios holocenos en la cuenca del Río Los Tártagos (Sierra Norte, Provincia de Córdoba): implicancias paleoclimáticas y geomorfológicas. Tesis doctoral, Facultad de Ciencias Exactas, Físicas y Naturales, Universidad Nacional de Córdoba, 2, p. 229. Unpublished.

Herrero, S.A., Piovano, E.L., Kirschbaum, A.M., 1998. Consideraciones cronológicas de las Areniscas ‘Cerro Colorado’ (Córdoba): criterios petrológicos y geomorfológicos. VII Reunión Argentina de Sedimentología, Salta, Actas, pp. 11–116.

Iniguez, A.M., Zalba, P.E., Andreis, R.R., 1990. Mineralogy and chemistry of Cambrian (?) paleosols, Tandilia System, Buenos Aires Province, Argentine. In: Farmer, V.C., Tardy, Y. (Eds.), Proccedings of the 9th International Clay Conference, Strasbourg, Sci. Géol., Mémoire, vol. 85, pp. 175–184.

Kirschbaum, A., 2002. La Meteorización en la Sierra del Aconquija, Tucumán (Argentina): Un Proceso Intenso a Escala Regional. IX Reunión Argentina de Sedimentología, Córdoba, Resúmenes, p. 94.

Kirschbaum, A., Herrero, S., Martínez, E., Roman Ross, G., Echevarrieta E., Pettinari G., Piovano, E., 2000. Perfiles de meteorización en relación a superficies de peneplanización en la Sierra Norte de Córdoba, Argentina. II Congreso Latinoamericano de Sedimentología y VIII Reunión Argentina de Sedimentología, Mar del Plata, Resúmenes, pp. 93–94.

Kirschbaum, A., Martínez, E., Pettinari, G., Herrero, S., 2002. Señales Mineralógicas y Geoquímicas de la Meteorización en Sierra Norte, Córdoba, Argentina. IX Reunión Argentina de Sedimentología, Córdoba, Resúmenes, p. 93.

Kirschbaum, A.M., Pérez, M.B., Baldo, E.G., Gordillo, D., 1997. Magmatismo oriental de las Sierras Pampeanas de Córdoba, Argentina: petrografía y geoquímica de los granitos de la Sierra de Macha. VIII Congreso Geológico Chileno, Actas II, 1319–1323.

Lira, R., Millone, H.A., Kirschbaum, A.M., Moreno, R., 1997. Calc-alkaline arc granitoid activity in the Sierra Norte—Ambargasta Ranges, Central Argentina. Journal of South American Earth Sciences 10 (2), 157–177.

R. Lira, R. Moreno, H.A. Millone, 1995. Sistemas de alteración porfíricos con sulfuros de cobre y molibdeno en el basamento eopaleozoico de la Sierra Norte de Córdoba, Argentina. V Congreso Nacional de Geología Económica, San Juan, Argentina, Actas, 426–430.

Lucero, H. N.,1969. Descripción geológica de las Hojas 16h, Pozo Grande y 17h, Chuña Huasi, Provincias de Córdoba y Santiago del Estero. Dirección Nacional de Geología y Minería, Buenos Aires, Boletín 107, 39.

Lucero Michaut, H. N.,1979. Sierras Pampeanas del norte de Córdoba, sur de Santiago del Estero, borde oriental de Catamarca y ángulo sudeste de Tucumán. Segundo Simposio de Geología Regional Argentina 1, Academia Nacional de Ciencias, Córdoba, pp. 293–348.

Middelburg, J.J., van der Weijden, C.H., Woittiez, J.R.W., 1988. Chemical processes affecting the mobility of major, minor and trace elements during weathering of granitic rocks. Chemical Geology 68, 253–273.

Millone, H.A., Moreno, R., Lira, R., Kirschbaum, A.M., 1994. An Ancient Collapse Breccia and Caldera-Type Structures Spatially Associated with Regional Mn–Ba Mineralization in the Sierra Norte Ranges, Córdoba Province, Argentina 9th Symposium of International Association on the Genesis of Ore Deposits, Beijing, China, vol. 1 1994 pp. 249–252.

Millot, G., 1964. Géologie des Argiles. Masson et Cie, Editeurs, Paris, p. 490.

Moore, D.M., Reynolds, R.C., 1997. X-Ray Diffraction and the Identification and Analysis of Clay Minerals, 2nd ed. Oxford Univ. Press, New York.

Nesbitt, H.W., 1979. Mobility and fractionation of rare earth elements during weathering of a granodiorite. Nature 279, 206–210.

Nesbitt, H.W., Markovics, G., 1997. Weathering of granodioritic crust, long-term storage of elements in weathering profiles, and petrogenesis of siliciclastic sediments. Geochimica et Cosmochimica Acta 61 (8), 1653–1670.

Nesbitt, H.W., Young, G.M., 1997. Sedimentation in the Venezuelan Basin, Circulation in the Caribbean Sea, and Onset of Northern Hemisphere Glaciation. Journal of Geology 105, 531–544.

M.S. O’Leary, A. Kirschbaum, G. Pettinari, G.R. Ross. Perfiles de meteorización en el granito de Achala, Córdoba, Argentina: aspectos petromineralógicos y geoquímicos. VII Reunión Argentina de Sedimentología, Salta Actas,, (1998) 79–89

J. Rabassa, M. Źrate, C. Camilión, T.Y. Patridge, R. Maud. Relieves relictuales de Tandilia y Ventania. IV Jornadas Geológicas Bonaerenses, Actas I, I (1995) 249–255

Ramos, V.A., 1999. Las Provincias Geológicas del Territorio Argentino. Instituto de Geología y Recursos Minerales. Buenos Aires. Geología Argentina, Anales 29 (3), 41–96.

Rapela, C.W., Pankhurst, R.J., Bonalumi, A.A., 1991. Edad y Geoquímica del Pórfido Granítico de Oncán, Sierra Norte de Córdoba, Sierras Pampeanas, Argentina. 6 Congreso Geológico Chileno Actas 6, 19–22.

Rapela, C.W., Pankhurst, C.R., Casquet, J., Baldo, E., Saavedra, J., Galindo, C., Fanning, C.M., 1998. In: Pankhurst, R.J., Rapela, C.W. (Eds.), The Pampean Orogeny of the Southern Proto-Andes:

Cambrian Continental Collision in the Sierras de Córdoba The Proto-Andean Margin of Gondwana, vol. 142. Geological Society, London, pp. 181–217.

Riggi, J.C., Feliu de Riggi, N.A., 1964. Meteorización de basaltos en Misiones. Asociación Geológica Argentina, Revista XIX (1), 57–70.

Ross, G.R., Kirschbaum, A.M., Guevara, S.R., Arribère, M.A., 1998. Procesos de meteorización en el granito de Achala, Sierra Grande de Córdoba: cambios químicos y mineralógicos. Revista de la Asociación Geológica Argentina 53 (4), 480–488.

Thieboult, F., Cremer, M., Debrabant, P., Foulon, J., Nielsen, O.B., Zimmerman, H., 1989. Analysis of Sedimentary Facies, Clay Mineralogy, and Geochemistry of the Neogene-Quaternary Sediments in Site 645, Bafin Bay Proceedings of Ocean Drilling Program, Scientific Results, vol. 105 1989. PP. 83–100.

Thiry, M., Schmitt, J.M., Simon - Coiçon, R., 1999. Problems, progress and future research concerning palaeoweathering and palaeosurfaces. In: Thiry, M. and Simon-Coinçon, R. (Eds.), Palaeoweathering, Palaeosurfaces and related Continental Deposits. International Association of Sedimetologists, Special Publication 27, 3-17.

Van der Weijden, C.H., van der Weijden, R.D., 1995. Mobility of major, minor and some redox-sensitive trace elements and rare-earth elements during weathering of four granitoids in central Portugal. Chemical Geology 125, 149–167.